

# SAM3-UNet: Simplified Adaptation of Segment Anything Model 3

Xinyu Xiong<sup>1\*</sup>, Zihuang Wu<sup>2\*</sup>, Lei Lu<sup>3,4\*</sup>, and Yufa Xia<sup>5,6</sup>

<sup>1</sup>Sun Yat-sen University <sup>2</sup>Jiangxi Normal University <sup>3</sup>Hainan University  
<sup>4</sup>Dalian University of Technology <sup>5</sup>Chizhou University <sup>6</sup>Wuhan University

**Abstract.** In this paper, we introduce SAM3-UNet, a simplified variant of Segment Anything Model 3 (SAM3), designed to adapt SAM3 for downstream tasks at a low cost. Our SAM3-UNet consists of three components: a SAM3 image encoder, a simple adapter for parameter-efficient fine-tuning, and a lightweight U-Net-style decoder. Preliminary experiments on multiple tasks, such as mirror detection and salient object detection, demonstrate that the proposed SAM3-UNet outperforms the prior SAM2-UNet and other state-of-the-art methods, while requiring less than 6 GB of GPU memory during training with a batch size of 12. The code is publicly available at <https://github.com/WZH0120/SAM3-UNet>.

## 1 Introduction

Foundation segmentation models, such as the Segment Anything Model series [9, 15, 2], have achieved remarkable success in recent years. Their large parameter scales and high-quality pre-training datasets endow them with strong out-of-domain generalization capabilities. Compared with SAM1 [9] and SAM2 [15], the recently proposed SAM3 [2] introduces support for concept (text) prompts and offers further advancements in interactive segmentation, providing the potential for more precise segmentation in a wide range of downstream tasks.

Although the text-prompting capability of SAM3 enables the segmentation of specific semantic categories without human involvement in real-time, it still exhibits several limitations. First, when processing objects with fine-grained structures [13], SAM3 often provides only coarse boundary predictions, achieving approximate localization rather than precise delineation. Second, for segmentation tasks involving context-dependent targets [19], text prompts may fail altogether. These limitations indicate that fine-tuning SAM3 to fully exploit its powerful pre-trained representations for downstream segmentation tasks remains an important and valuable research direction.

In this paper, we propose SAM3-UNet, a simplified variant of SAM3 that enables efficient fine-tuning for downstream segmentation tasks. The advantages of SAM3-UNet are summarized as follows:

---

\* Authors contributed equally to this work.

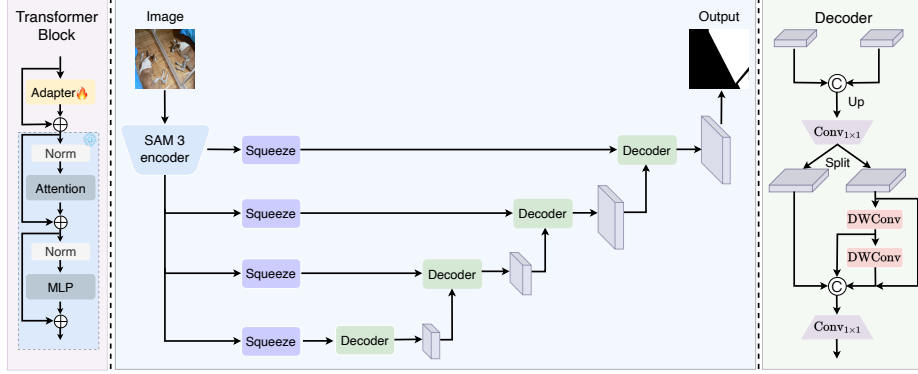


**Fig. 1.** Overview of the proposed SAM3-UNet. For simplicity, we show only the decoder block where feature fusion is available.

- **Compact.** We retain only the image encoder of SAM3 and remove the remaining components, yielding a more concise and easily extensible framework while preserving strong performance.
- **Efficient.** By relaxing the resolution constraints and adopting a lightweight decoder, our framework lowers the hardware requirements for fine-tuning.
- **Effective.** Experiments on two benchmarks demonstrate that our framework outperforms existing methods.

## 2 Method

The overall architecture of SAM3-UNet is shown in Fig. 1. It consists of an adapter-enhanced SAM3 image encoder and a lightweight U-Net-style decoder.

### 2.1 SAM3 Encoder

SAM3 employs a ViT-style [3] perception encoder [1] as its image encoder, rather than continuing the Hiera [17] architecture used in SAM2. In terms of scale, the vision encoder of SAM3 lies between the standard ViT-L and ViT-H, featuring a total of 446M parameters, which makes full fine-tuning computationally expensive. To address this, we design a simple yet effective parameter-efficient fine-tuning strategy. Specifically, we freeze all original ViT parameters and insert learnable adapter [8] modules before each transformer block. Each adapter adopts a bottleneck structure composed of a downsampling layer, a GELU function, an upsampling layer, and a final GELU function.

In our previous work, SAM2-UNet [23], the hierarchical encoder features are first enhanced using receptive-field blocks and then decoded by a standard U-Net [16] decoder composed of dual convolutional blocks. In this work, considering that the SAM3 encoder is non-hierarchical and larger than that of SAM2, we make the following modifications. First, for the ViT output embedding of size



**Fig. 2.** Visualization results on mirror detection.



**Fig. 3.** Visualization results on salient object detection.

( $H/14$ ,  $W/14$ ) with 1024 channels, where  $H$  and  $W$  denote the input image height and width, respectively, we apply four  $1 \times 1$  convolutions to compress it into four lightweight feature maps, each with 128 channels. We then employ bilinear interpolation to resize these feature maps to ( $H/4$ ,  $W/4$ ), ( $H/8$ ,  $W/8$ ), ( $H/16$ ,  $W/16$ ), and ( $H/32$ ,  $W/32$ ), respectively. These resized features are treated as hierarchical representations and subsequently fed into a lightweight decoder for further learning.

## 2.2 Lightweight Decoder

In SAM2-UNet, the decoder adopts a standard double-convolution block design. Although this structure has been widely validated for its reliability and segmentation accuracy, its computational efficiency and convergence speed are inferior to those of more modern architectures. Therefore, while striving to maintain simplicity, we redesign a lightweight block to replace the original double-convolution block in the decoder.

Specifically, to develop a simple yet efficient lightweight block, we incorporate three key design principles: bottlenecking, depthwise separable convolution, and feature splitting. Given an input feature map, we first apply a set of  $1 \times 1$  Conv-BN-GELU layers to reduce the channel dimension from  $C$  to  $C/4$ . The reduced feature is then split evenly along the channel dimension into two parts, each with  $C/8$  channels. The second part is sequentially processed by two  $3 \times 3$  depthwise convolution blocks, generating the third and fourth parts. Finally, all four parts are concatenated along the channel dimension and passed through

**Table 1.** Mirror detection performance on MSD [26] and PMD [12] datasets.

Methods	MSD			PMD		
	$IoU$	$F$	MAE	$IoU$	$F$	MAE
MirrorNet [26]	0.790	0.857	0.065	0.585	0.741	0.043
SANet [6]	0.798	0.877	0.054	0.668	0.795	0.032
HetNet [7]	0.828	0.906	0.043	0.690	0.814	0.029
DPRNet [28]	0.866	/	0.033	0.721	/	0.026
S2MD [18]	0.871	0.936	0.032	0.698	0.846	0.024
SAM2-UNet [23]	0.918	0.957	0.022	0.728	0.826	0.027
<b>SAM3-UNet</b>	<b>0.943</b>	<b>0.972</b>	<b>0.014</b>	<b>0.804</b>	<b>0.884</b>	<b>0.017</b>

**Table 2.** Salient object detection performance on DUTS-TE [19], DUT-OMRON [25], HKU-IS [10], PASCAL-S [11] and ECSSD [24] datasets.

Methods	DUTS-TE			DUT-OMRON			HKU-IS			PASCAL-S			ECSSD		
	$S_\alpha$	$E_\phi$	MAE	$S_\alpha$	$E_\phi$	MAE	$S_\alpha$	$E_\phi$	MAE	$S_\alpha$	$E_\phi$	MAE	$S_\alpha$	$E_\phi$	MAE
U2Net [14]	0.874	0.884	0.044	0.847	0.872	0.054	0.916	0.948	0.031	0.844	0.850	0.074	0.928	0.925	0.033
ICON [29]	0.889	0.914	0.037	0.845	0.879	0.057	0.920	0.959	0.029	0.861	0.893	0.064	0.929	0.954	0.032
EDN [22]	0.892	0.925	0.035	0.850	0.877	0.049	0.924	0.955	0.026	0.865	0.902	0.062	0.927	0.951	0.032
MENet [20]	0.905	0.937	0.028	0.850	0.891	0.045	0.927	0.966	0.023	0.872	0.913	0.054	0.928	0.954	0.031
UGRANet [27]	0.931	<b>0.964</b>	0.022	0.878	0.911	0.045	<b>0.945</b>	<b>0.978</b>	<b>0.019</b>	0.892	0.934	0.046	<b>0.950</b>	<b>0.975</b>	0.020
SAM2-UNet [23]	0.934	0.959	0.020	0.884	0.912	0.039	0.941	0.971	<b>0.019</b>	0.894	0.931	0.043	<b>0.950</b>	0.970	0.020
<b>SAM3-UNet</b>	<b>0.936</b>	<b>0.964</b>	<b>0.019</b>	<b>0.895</b>	<b>0.921</b>	<b>0.034</b>	0.939	0.968	0.020	<b>0.904</b>	<b>0.939</b>	<b>0.038</b>	<b>0.950</b>	0.970	<b>0.019</b>

another set of  $1 \times 1$  Conv-BN-GELU layers to expand the channels to the desired output dimension.

### 3 Experiments

#### 3.1 Datasets

We conduct experiments on the following two segmentation benchmarks:

**Mirror Detection.** This benchmark conduct two sperate datasets. Following the official dataset split, for the MSD [26] dataset, 3,063 images are used for training and 955 images are used for testing. For the PMD [12] dataset, 5,096 images are used for training and 571 are used for testing. We report results using IoU, F-measure (F), and mean absolute error (MAE).

**Salient Object Detection.** This benchmark consists five datasets in total. Following the common practice, the training set is DUTS-TR [19], which contains 10,553 images. The testing set contains five subsets: DUTS-TE [19] (5,019 images), DUT-OMRON [25] (5,168 images), HKU-IS [10] (4,447 images), PASCAL-S [11] (850 images), ECSSD [24] (1,000 images). We report results using S-measure [4] ( $S_\alpha$ ), mean E-measure [5] ( $E_\phi$ ), and mean absolute error (MAE).

### 3.2 Implementation Details

Our method is implemented in PyTorch and trained on a NVIDIA RTX 4090 GPU with 24 GB of memory. We use the AdamW optimizer with an initial learning rate of 0.0002 and apply cosine learning rate decay to stabilize training. The overall loss function consists of a weighted cross-entropy loss [21] ( $\mathcal{L}_{\text{BCE}}^w$ ) and a weighted IoU loss [21] ( $\mathcal{L}_{\text{IoU}}^w$ ). Two data augmentation strategies, including random horizontal and vertical flipping, are employed during training. The input resolutions are set to  $(H, W) = (336, 336)$ . The bottleneck of the adapter module is set to 32 channels. All models are trained with a batch size of 12 for 20 epochs across different tasks.

### 3.3 Result Analysis

**Results on Mirror Detection.** As reported in Table 1, the proposed SAM3-UNet establishes a new state-of-the-art on both MSD and PMD benchmarks. It improves the best IoU from 0.918 to 0.943 on MSD (2.5% improvement) and from 0.728 to 0.804 on PMD (7.6% improvement). Some visual results are shown in Fig. 2. Our method is better at handling irregular shapes (row 1, 3) and hidden targets (row 2).

**Results on Salient Object Detection.** As reported in Table 2, taking the S-measure as an example, the proposed SAM3-UNet achieves better or comparable results on four out of the five datasets. The most significant improvement is observed on the DUT-OMRON dataset, where it further surpasses the second-best method, SAM2-UNet, by 1.1%. Some visual results are shown in Fig. 3. Our method more accurately identifies salient objects in cluttered environments (row 1, 2).

## 4 Conclusion

In this paper, we propose SAM3-UNet, a simple yet effective U-shaped framework that enables versatile segmentation through a simplified adaptation of Segment Anything Model 3. By retaining only the SAM3 image encoder, introducing lightweight adapters for parameter-efficient fine-tuning, and designing an efficient U-Net-style decoder, SAM3-UNet achieves strong segmentation performance with substantially reduced computational cost. Extensive experiments on multiple benchmarks demonstrate that our framework not only surpasses existing methods but also offers a practical and scalable solution for a wide range of downstream segmentation tasks.

## References

1. Bolya, D., Huang, P.Y., Sun, P., Cho, J.H., Madotto, A., Wei, C., Ma, T., Zhi, J., Rajasegaran, J., Rasheed, H., et al.: Perception encoder: The best visual embeddings are not at the output of the network. arXiv preprint arXiv:2504.13181 (2025)

2. Carion, N., Gustafson, L., Hu, Y.T., Debnath, S., Hu, R., Suris, D., Ryali, C., Alwala, K.V., Khedr, H., Huang, A., et al.: Sam 3: Segment anything with concepts. arXiv preprint arXiv:2511.16719 (2025)
3. Dosovitskiy, A., Beyer, L., Kolesnikov, A., Weissenborn, D., Zhai, X., Unterthiner, T., Dehghani, M., Minderer, M., Heigold, G., Gelly, S., Uszkoreit, J., Houlsby, N.: An image is worth 16x16 words: Transformers for image recognition at scale. In: ICLR (2021)
4. Fan, D.P., Cheng, M.M., Liu, Y., Li, T., Borji, A.: Structure-measure: A new way to evaluate foreground maps. In: ICCV. pp. 4548–4557 (2017)
5. Fan, D.P., Ji, G.P., Qin, X., Cheng, M.M.: Cognitive vision inspired object segmentation metric and loss function. *Scientia Sinica Informationis* **6**(6), 5 (2021)
6. Guan, H., Lin, J., Lau, R.W.: Learning semantic associations for mirror detection. In: CVPR. pp. 5941–5950 (2022)
7. He, R., Lin, J., Lau, R.W.: Efficient mirror detection via multi-level heterogeneous learning. In: AAAI. vol. 37, pp. 790–798 (2023)
8. Houlsby, N., Giurgiu, A., Jastrzebski, S., Morrone, B., De Laroussilhe, Q., Gesmundo, A., Attariyan, M., Gelly, S.: Parameter-efficient transfer learning for nlp. In: ICML. pp. 2790–2799. PMLR (2019)
9. Kirillov, A., Mintun, E., Ravi, N., Mao, H., Rolland, C., Gustafson, L., Xiao, T., Whitehead, S., Berg, A.C., Lo, W.Y., et al.: Segment anything. In: ICCV. pp. 4015–4026 (2023)
10. Li, G., Yu, Y.: Visual saliency based on multiscale deep features. In: CVPR. pp. 5455–5463 (2015)
11. Li, Y., Hou, X., Koch, C., Rehg, J.M., Yuille, A.L.: The secrets of salient object segmentation. In: CVPR. pp. 280–287 (2014)
12. Lin, J., Wang, G., Lau, R.W.: Progressive mirror detection. In: CVPR. pp. 3697–3705 (2020)
13. Qin, X., Dai, H., Hu, X., Fan, D.P., Shao, L., Van Gool, L.: Highly accurate dichotomous image segmentation. In: European Conference on Computer Vision. pp. 38–56. Springer (2022)
14. Qin, X., Zhang, Z., Huang, C., Dehghan, M., Zaiane, O.R., Jagersand, M.: U2-net: Going deeper with nested u-structure for salient object detection. *Pattern Recognition* **106**, 107404 (2020)
15. Ravi, N., Gabeur, V., Hu, Y.T., Hu, R., Ryali, C., Ma, T., Khedr, H., Rädle, R., Rolland, C., Gustafson, L., et al.: Sam 2: Segment anything in images and videos. In: ICLR (2025)
16. Ronneberger, O., Fischer, P., Brox, T.: U-net: Convolutional networks for biomedical image segmentation. In: MICCAI. pp. 234–241. Springer (2015)
17. Ryali, C., Hu, Y.T., Bolya, D., Wei, C., Fan, H., Huang, P.Y., Aggarwal, V., Chowdhury, A., Poursaeed, O., Hoffman, J., et al.: Hiera: A hierarchical vision transformer without the bells-and-whistles. In: ICML. pp. 29441–29454. PMLR (2023)
18. Shao, Z., Chen, R., Shi, X., Liu, B., Li, C., Ma, L., Yeung, D.Y.: Mirror detection via multi-directional similarity perception and spectral saliency enhancement. *IEEE Transactions on Circuits and Systems for Video Technology* (2025)
19. Wang, L., Lu, H., Wang, Y., Feng, M., Wang, D., Yin, B., Ruan, X.: Learning to detect salient objects with image-level supervision. In: CVPR. pp. 136–145 (2017)
20. Wang, Y., Wang, R., Fan, X., Wang, T., He, X.: Pixels, regions, and objects: Multiple enhancement for salient object detection. In: CVPR. pp. 10031–10040 (2023)

21. Wei, J., Wang, S., Huang, Q.: F<sup>3</sup>net: fusion, feedback and focus for salient object detection. In: AAAI. pp. 12321–12328 (2020)
22. Wu, Y.H., Liu, Y., Zhang, L., Cheng, M.M., Ren, B.: Edn: Salient object detection via extremely-downsampled network. *IEEE Transactions on Image Processing* **31**, 3125–3136 (2022)
23. Xiong, X., Wu, Z., Tan, S., Li, W., Tang, F., Chen, Y., Li, S., Ma, J., Li, G.: Sam2-unet: Segment anything 2 makes strong encoder for natural and medical image segmentation. *arXiv preprint arXiv:2408.08870* (2024)
24. Yan, Q., Xu, L., Shi, J., Jia, J.: Hierarchical saliency detection. In: CVPR. pp. 1155–1162 (2013)
25. Yang, C., Zhang, L., Lu, H., Ruan, X., Yang, M.H.: Saliency detection via graph-based manifold ranking. In: CVPR. pp. 3166–3173 (2013)
26. Yang, X., Mei, H., Xu, K., Wei, X., Yin, B., Lau, R.W.: Where is my mirror? In: ICCV. pp. 8809–8818 (2019)
27. Yuan, Y., Gao, P., Dai, Q., Qin, J., Xiang, W.: Uncertainty guided refinement for fine-grained salient object detection. *IEEE Transactions on Image Processing* (2025)
28. Zha, M., Fu, F., Pei, Y., Wang, G., Li, T., Tang, X., Yang, Y., Shen, H.T.: Dual domain perception and progressive refinement for mirror detection. *IEEE Transactions on Circuits and Systems for Video Technology* (2024)
29. Zhuge, M., Fan, D.P., Liu, N., Zhang, D., Xu, D., Shao, L.: Salient object detection via integrity learning. *IEEE Transactions on Pattern Analysis and Machine Intelligence* **45**(3), 3738–3752 (2022)